

Global trait–environment relationships of plant communities

Helge Bruelheide, Jurgen Dengler, Oliver Purschke, Jonathan Roger Michel Henri Lenoir, Borja Jiménez-Alfaro, Stephan Hennekens, Zoltán Botta-Dukát, Milan Chytrý, Richard Field, Florian Jansen, et al.

► To cite this version:

Helge Bruelheide, Jurgen Dengler, Oliver Purschke, Jonathan Roger Michel Henri Lenoir, Borja Jiménez-Alfaro, et al.. Global trait–environment relationships of plant communities. Nature Ecology & Evolution, 2018, 2 (12), pp.1906-1917. 10.1038/s41559-018-0699-8. hal-02352596

HAL Id: hal-02352596 https://hal.science/hal-02352596v1

Submitted on 19 Feb2025

HAL is a multi-disciplinary open access archive for the deposit and dissemination of scientific research documents, whether they are published or not. The documents may come from teaching and research institutions in France or abroad, or from public or private research centers. L'archive ouverte pluridisciplinaire **HAL**, est destinée au dépôt et à la diffusion de documents scientifiques de niveau recherche, publiés ou non, émanant des établissements d'enseignement et de recherche français ou étrangers, des laboratoires publics ou privés. 1 Title:

2 Global trait–environment relationships of plant communities

3

4 **One Sentence Summary:** Trait composition of plant communities across the globe is

- 5 captured by two main dimensions and is probably shaped by environmental or biotic filtering,
- 6 but is only weakly related to global climate and soil gradients.

7 Authors:

Helge Bruelheide^{1,2,*}, Jürgen Dengler^{2,3,4}, Oliver Purschke^{1,2}, Jonathan Lenoir⁵, Borja 8 Jiménez-Alfaro^{6,1,2}, Stephan M. Hennekens⁷, Zoltán Botta-Dukát⁸, Milan Chytrý⁹, Richard 9 Field¹⁰, Florian Jansen¹¹, Jens Kattge^{2,12}, Valério D. Pillar¹³, Franziska Schrodt^{10,12}, Miguel D. 10 Mahecha^{2,12}, Robert K. Peet¹⁴, Brody Sandel¹⁵, Peter van Bodegom¹⁶, Jan Altman¹⁷, Esteban 11 Alvarez Davila¹⁸, Mohammed A.S. Arfin Khan^{19,20}, Fabio Attorre²¹, Isabelle Aubin²², 12 Christopher Baraloto²³, Jorcely G. Barroso²⁴, Marijn Bauters²⁵, Erwin Bergmeier²⁶, Idoia 13 Biurrun²⁷, Anne D. Bjorkman²⁸, Benjamin Blonder^{29,30}, Andraž Čarni^{31,32}, Luis Cayuela³³, 14 Tomáš Černý³⁴, J. Hans C. Cornelissen³⁵, Dylan Craven^{2,36}, Matteo Dainese³⁷, Géraldine 15 Derroire³⁸, Michele De Sanctis²¹, Sandra Díaz³⁹, Jiří Doležal¹⁷, William Farfan-Rios^{40,41}, Ted 16 R. Feldpausch⁴², Nicole J. Fenton⁴³, Eric Garnier⁴⁴, Greg R. Guerin⁴⁵, Alvaro G. Gutiérrez⁴⁶, 17 Sylvia Haider^{1,2}, Tarek Hattab⁴⁷, Greg Henry⁴⁸, Bruno Hérault^{49,50}, Pedro Higuchi⁵¹, Norbert 18 Hölzel⁵², Jürgen Homeier⁵³, Anke Jentsch²⁰, Norbert Jürgens⁵⁴, Zygmunt Kącki⁵⁵, Dirk N. 19 Karger^{56,57}, Michael Kessler⁵⁶, Michael Kleyer⁵⁸, Ilona Knollová⁹, Andrey Y. Korolyuk⁵⁹, 20 Ingolf Kühn^{36,1,2}, Daniel C. Laughlin^{60,61}, Frederic Lens⁶², Jacqueline Loos⁶³, Frédérique 21 Louault⁶⁴, Mariyana I. Lyubenova⁶⁵, Yadvinder Malhi⁶⁶, Corrado Marcenò²⁷, Maurizio 22 Mencuccini^{67,68}, Jonas V. Müller⁶⁹, Jérôme Munzinger⁷⁰, Isla H. Myers-Smith⁷¹, David A. 23 Neill⁷², Ülo Niinemets⁷³, Kate H. Orwin⁷⁴, Wim A. Ozinga^{7,75}, Josep Penuelas^{68,73,76}, Aaron 24 Pérez-Haase^{77,78}, Petr Petřík¹⁷, Oliver L. Phillips⁷⁹, Meelis Pärtel⁸⁰, Peter B. Reich^{81,82}, 25 Christine Römermann^{2,83}, Arthur V. Rodrigues⁸⁴, Francesco Maria Sabatini^{1,2}, Jordi 26 Sardans^{68,76}, Marco Schmidt⁸⁵, Gunnar Seidler¹, Javier Eduardo Silva Espejo⁸⁶, Marcos 27 Silveira⁸⁷, Anita Smyth⁴⁵, Maria Sporbert^{1,2}, Jens-Christian Svenning²⁸, Zhiyao Tang⁸⁸, 28 Raquel Thomas⁸⁹, Ioannis Tsiripidis⁹⁰, Kiril Vassilev⁹¹, Cyrille Violle⁴⁴, Risto Virtanen^{2,92,93}, 29 Evan Weiher⁹⁴, Erik Welk^{1,2}, Karsten Wesche^{2,95,96}, Marten Winter², Christian Wirth^{2,12,97}, 30 Ute Jandt^{1,2} 31

32 Affiliations:

¹ Martin Luther University Halle-Wittenberg, Institute of Biology/Geobotany and Botanical

34 Garden, Am Kirchtor 1, 06108 Halle, Germany

²German Centre for Integrative Biodiversity Research (iDiv) Halle-Jena-Leipzig, Deutscher

36 Platz 5e, 04103 Leipzig, Germany

- ³Zurich University of Applied Sciences (ZHAW), Institute of Natural Resource Sciences
- 38 (IUNR), Research Group Vegetation Ecology, Grüentalstr. 14, Postfach, 8820 Wädenswil,
- 39 Switzerland
- ⁴University of Bayreuth, Bayreuth Center of Ecology and Environmental Research
- 41 BayCEER, Plant Ecology, Universitätsstr. 30, 95447 Bayreuth, Germany
- 42 ⁵ CNRS, Université de Picardie Jules Verne, UR «Ecologie et Dynamique des Systèmes
- 43 Anthropisés» (EDYSAN, UMR 7058 CNRS-UPJV), 1 rue des Louvels, 80037 Amiens Cedex
- 44 1, France
- 45 ⁶ Research Unit of Biodiversity (CSIC/UO/PA), University of Oviedo, Campus de Mieres, c/
- 46 Gonzalo Gutiérrez Quirós s/n 33600 Mieres, Spain
- ⁴⁷ ⁷ Wageningen Environmental Research (Alterra), Team Vegetation, Forest and Landscape
- 48 Ecology, PO Box 47, 6700 AA Wageningen, The Netherlands
- ⁸ MTA Centre for Ecological Research, GINOP Sustainable Ecosystems Group, 8237 Tihany,
- 50 Klebesberg Kuno u. 3, Hungary
- ⁹ Masaryk University, Department of Botany and Zoology, Kotlářská 2, 611 37 Brno, Czech
- 52 Republic
- ¹⁰ University of Nottingham, School of Geography, University Park, Nottingham, NG7 2RD,
- 54 United Kingdom
- ¹¹ University of Rostock, Faculty for Agricultural and Environmental Sciences, Justus-von-
- 56 Liebig-Weg 6, 18059 Rostock, Germany
- ¹² Max Planck Institute for Biogeochemistry, Hans-Knöll-Str. 10, 07745 Jena, Gemany
- ¹³ Universidade Federal do Rio Grande do Sul, Department of Ecology, Porto Alegre, RS,
- 59 91501-970, Brazil
- ¹⁴ University of North Carolina at Chapel Hill, Department of Biology, Chapel Hill, NC
- 61 27599-3280, USA
- ¹⁵ Santa Clara University, Department of Biology, Santa Clara CA 95053, USA
- ¹⁶ Leiden University, Institute of Environmental Sciences, Department Conservation Biology,
- Einsteinweg 2, 2333 CC Leiden, The Netherlands
- ¹⁷ Institute of Botany of the Czech Academy of Sciences, Zámek 1, 252 43 Průhonice, Czech
 Republic
- ¹⁸ Escuela de Ciencias Agropecuarias y Ambientales ECAPMA, Universidad Nacional
- Abierta y a Distancia –UNAD, Sede José Celestino Mutis, Calle 14S #14, Bogotá
- ¹⁹ Shahjalal University of Science and Technology, Department of Forestry and
- 70 Environmental Science, Sylhet, 3114, Bangladesh

- ²⁰ University of Bayreuth, Bayreuth Center of Ecology and Environmental Research
- 72 BayCEER, Department of Disturbance Ecology, Universitätsstr. 30, 95447 Bayreuth,
- 73 Germany
- ²¹ Sapienza University of Rome, Department of Environmental Biology, P.le Aldo Moro 5,
- 75 00185 Rome, Italy
- ²² Great Lakes Forestry Centre, Canadian Forest Service, Natural Resources Canada, 1219
- 77 Queen St. East, Sault Ste Marie, ON, P6A 2E5, Canada
- ²³ Florida International University, Department of Biological Sciences, International Center
- 79 for Tropical Botany (ICTB), 11200 SW 8th Street, OE 243 Miami, FL 33199, USA
- 80 ²⁴ Universidade Federal do Acre, Campus de Cruzeiro do Sul, Acre, Brazil.
- 81 ²⁵ Ghent University, Faculty of Bioscience Engineering, Department of Applied Analytical
- and Physical Chemistry, ISOFYS, Coupure Links 653, 9000 Gent, Belgium
- ²⁶ University of Göttingen, Albrecht von Haller Institute of Plant Sciences, Vegetation
- 84 Analysis & Plant Diversity, Untere Karspüle 2, 37073 Göttingen, Germany
- ²⁷ University of the Basque Country UPV/EHU, Apdo. 644, 48080 Bilbao, Spain
- ²⁸ Aarhus University, Department of Bioscience, Section for Ecoinformatics & Biodiversity,
- 87 Ny Munkegade 114, 8000 Aarhus C, Denmark
- ²⁹ University of Oxford, Environmental Change Institute, School of Geography and the
- 89 Environment, South Parks Road, Oxford OX1 3QY, United Kingdom
- ³⁰ Rocky Mountain Biological Laboratory, PO Box 519, Crested Butte, Colorado, 81224 USA
- ³¹ Scientific Research Center of the Slovenian Academy of Sciences and Arts, Institute of
- 92 Biology, Novi trg 2, SI 1001 Ljubljana p. box 306, Slovenia
- ³² University of Nova Gorica, 5000 Nova Gorica, Slovenia
- ³³ Universidad Rey Juan Carlos, Department of Biology, Geology, Physics and Inorganic
- 95 Chemistry, c/ Tulipán s/n, 28933 Móstoles, Madrid, Spain
- ³⁴ Czech University of Life Sciences, Faculty of Forestry and Wood Science, Department of
- 97 Forest Ecology, Kamýcká 1176, 16521, Praha 6 Suchdol, Czech Republic
- 98 ³⁵ Vrije Universiteit Amsterdam, Faculty of Science, Department of Ecological Science, De
- 99 Boelelaan 1085, 1081 HV Amsterdam, The Netherlands
- 100 ³⁶ Helmholtz Centre for Environmental Research UFZ, Dept. Community Ecology,
- 101 Theodor-Lieser-Str. 4, 06120 Halle, Germany
- ³⁷ University of Würzburg, Department of Animal Ecology and Tropical Biology, Am
- 103 Hubland, 97074 Würzburg, Germany
- ³⁸ Cirad, UMR EcoFoG, Campus Agronomique, 97310 Kourou, French Guiana

- ³⁹ Instituto Multidisciplinario de Biología Vegetal (IMBIV), CONICET and FCEFyN,
- 106 Universidad Nacional de Córdoba, Casilla de Correo 495, 5000 Córdoba, Argentina.
- ⁴⁰ Wake Forest University, Department of Biology, Winston Salem, North Carolina, USA
- ⁴¹ Universidad Nacional de San Antonio Abad del Cusco, Herbario Vargas (CUZ), Cusco,
- 109 Peru
- ⁴² University of Exeter, College of Life and Environmental Sciences, Geography, Exeter, EX4
- 111 4RJ, United Kingdom.
- ⁴³ Université du Québec en Abitibi-Témiscamingue, Institut de recherche sur les forêts, 445
- 113 Boul. de l'Université, Rouyn-Noranda, Qc J9X 4E5, Canada
- ⁴⁴ CNRS Université de Montpellier Université Paul-Valéry Montpellier EPHE, Centre
- d'Ecologie Fonctionnelle et Evolutive (UMR5175), 34293 Montpellier Cedex 5, France
- ⁴⁵ University of Adelaide, Terrestrial Ecosystem Research Network, School of Biological
- 117 Sciences, Adelaide, South Australia, 5005 Australia
- ⁴⁶ Universidad de Chile, Facultad de Ciencias Agronómicas, Departamento de Ciencias
- 119 Ambientales y Recursos Naturales Renovables, Av. Santa Rosa 11315, La Pintana 8820808,
- 120 Santiago, Chile
- ⁴⁷ IFREMER (Institut Français de Recherche pour l'Exploitation de la MER) UMR 248
- 122 MARBEC (CNRS, IFREMER, IRD, UM), 34203 Sète cedex, France
- ⁴⁸ University of British Columbia, The Department of Geography, 1984 West Mall,
- 124 Vancouver, BC V6T 1Z2, Canada
- ⁴⁹ INPHB (Institut National Polytechnique Félix Houphouët-Boigny), BP 1093,
- 126 Yamoussoukro, Ivory Coast
- ⁵⁰Cirad, University Montpellier, UR Forests & Societies, Montpellier, France
- ⁵¹ Universidade do Estado de Santa Catarina (UDESC), Departamento de Engenharia
- 129 Florestal, Av Luiz de Camões, 2090 Conta Dinheiro, Lages SC, 88.520 000, Brazil
- ⁵² University of Münster, Institute of Landscape Ecology, Heisenbergstr. 2, 48149 Münster,
- 131 Germany
- ⁵³ University of Göttingen, Plant Ecology and Ecosystems Research, Untere Karspüle 2,
- 133 37073 Göttingen, Germany
- ⁵⁴ University of Hamburg, Biodiversity, Biocenter Klein Flottbek and Botanical Garden,
- 135 Ohnhorststr. 18, 22609 Hamburg, Germany
- 136 ⁵⁵ University of Wroclaw, Institute of Environmental Biology, Department of Vegetation
- 137 Ecology, Przybyszewskiego 63, 51-148 Wrocław, Poland

- ⁵⁶ University of Zurich, Department of Systematic and Evolutionary Botany, Zollikerstrasse
- 139 107, 8008 Zurich, Switzerland
- ⁵⁷ Swiss Federal Research Institute WSL, Zürcherstrasse 111, 8903 Birmensdorf, Switzerland.
- ⁵⁸ University of Oldenburg, Institute of Biology and Environmental Sciences, Landscape
- 142 Ecology Group, Carl-von-Ossietzky Strasse 9-11, 26111 Oldenburg, Germany
- ⁵⁹ Central Siberian Botanical Garden SB RAS, Zolotodolinskaya str. 101, Novosibirsk,
- 144 630090, Russia
- ⁶⁰ University of Waikato, Environmental Research Institute, School of Science, Private Bag
- 146 3105, Hamilton 3240, New Zealand
- ⁶¹ University of Wyoming, Department of Botany, Laramie, Wyoming, USA
- ⁶² Leiden University, Naturalis Biodiversity Center, P.O. Box 9517, 2300RA Leiden, The
- 149 Netherlands
- ⁶³ Agroecology, University of Göttingen, Grisebachstrasse 6, 37077 Göttingen, Germany
- ⁶⁴ INRA, VetAgro Sup, UMR Ecosystème Prairial, 63000 Clermont-Ferrand, France
- ⁶⁵ University of Sofia, Faculty of Biology, Department of Ecology and Environmental
- 153 Protection, 1164 Sofia, 8 Dragan Tsankov Av., Bulgaria
- ⁶⁶ University of Oxford, Environmental Change Institute, School of Geography and the
- 155 Environment, South Parks Road, Oxford, OX1 3QY, United Kingdom
- 156 ⁶⁷ ICREA Pg. Lluís Companys 23, 08010 Barcelona, Spain
- ⁶⁸ CREAF, Cerdanyola del Vallès, 08193 Barcelona, Catalonia, Spain
- ⁶⁹ Royal Botanic Gardens Kew, Millennium Seed Bank, Conservation Science, Wakehurst
- 159 Place, Ardingly, RH17 6TN, United Kingdom
- ⁷⁰ AMAP, IRD, CNRS, INRA, Université Montpellier, 34000 Montpellier, France
- ⁷¹ University of Edinburgh, School of GeoSciences, Edinburgh EH9 3FF, United Kingdom
- 162 ⁷² Universidad Estatal Amazónica, Conservación y Manejo de Vida Silvestre, Paso lateral km
- 163 2¹/₂ via a Napo Puyo, Pastaza, Ecuador
- ⁷³ Estonian University of Life Science, Department of Crop Science and Plant Biology,
- 165 Kreutzwaldi 1, 51014, Tartu, Estonia
- 166 ⁷⁴ Landcare Research, PO Box 69040, Lincoln 7640, New Zealand
- ⁷⁵ Radboud University Nijmegen, Institute for Water and Wetland Research, 6500 GL
- 168 Nijmegen, The Netherlands
- ⁷⁶ CSIC, Global Ecology Unit, CREAF-CEAB-UAB, Cerdanyola del Vallès, 08193
- 170 Barcelona, Catalonia, Spain

- ⁷⁷ University of Barcelona, Faculty of Biology, Department of Evolutionary Biology, Ecology
- and Environmental Sciences, Av. Diagonal 643, 08028, Barcelona, Spain
- ⁷⁸ Center for Advanced Studies of Blanes, Spanish Research Council
- 174 (CEAB-CSIC), 17300 Blanes, Spain
- ⁷⁹ University of Leeds, School of Geography, Leeds LS2 9JT, United Kingdom
- 176 ⁸⁰ University of Tartu, Ülikooli 18, 50090 Tartu, Estonia
- ⁸¹ University of Minnesota, Department of Forest Recourses, 220F Green Hall,
- 178 1530 Cleveland Avenue North, St. Paul, MN 55108, USA
- ⁸² Western Sydney University, Hawkesbury Institute for the Environment, New South Wales
- 180 2751, Australia
- 181 ⁸³ Friedrich Schiller University Jena, Institute of Systematic Botany, Philosophenweg 16,
- 182 07743 Jena, Germany
- 183 ⁸⁴ Universidade Regional de Blumenau, Departamento de Engenharia Florestal, Rua São
- 184 Paulo, 3250, 89030-000 Blumenau-Santa Catarina, Brazil
- 185 ⁸⁵ Senckenberg Biodiversity and Climate Research Centre (BiK-F), Data and Modelling
- 186 Centre, Senckenberganlage 25, 60325 Frankfurt am Main, Germany
- 187 ⁸⁶ University of La Serena , Department of Biology, La Serena, Chile
- 188 ⁸⁷ Universidade Federal do Acre, Museu Universitário / Centro de Ciências Biológicas e da
- 189 Natureza / Laboratório de Botânica e Ecologia Vegetal, BR 364, Km 04 Distrito Industrial -
- 190 69915-559 Rio Branco-AC, Brazil
- ⁸⁸ Peking University, College of Urban and Environmental Sciences, Yiheyuan Rd. 5, 100871,
- 192 Beijing, China
- ⁸⁹ Iwokrama International Centre for Rain Forest Conservation and Development, 77 High
- 194 Street, Kingston, Georgetown, Guyana
- ⁹⁰ Aristotle University of Thessaloniki, School of Biology, Department of Botany, 54124
- 196 Greece
- ⁹¹ Bulgarian Academy of Sciences, Institute of Biodiversity and Ecosystem Research, 23
- 198 Acad. G. Bonchev Str., 1113 Sofia, Bulgaria
- ⁹² Helmholtz Center for Environmental Research UFZ, Department of Physiological
- 200 Diversity, Permoserstraße 15, Leipzig 04318, Germany
- ⁹³ University of Oulu, Department of Ecology & Genetics, PO Box 3000, FI-90014, Finland
- ⁹⁴ University of Wisconsin Eau Claire, Department of Biology, Eau Claire, WI 54702-4004,
- 203 USA

- ⁹⁵ Senckenberg Museum of Natural History Görlitz, P.O. Box 300154, 02806 Görlitz,
- 205 Germany
- ⁹⁶ TU Dresden, International Institute (IHI) Zittau, Markt 23, 02763 Zittau, Germany
- ⁹⁷ University of Leipzig, Systematic Botany and Functional Biodiversity, Johannisallee 21–
- 208 23, 04103 Leipzig, Germany
- 209
- 210 ^{*} Corresponding author
- 211
- 212

213 Abstract:

Plant functional traits directly affect ecosystem functions. At the species level, trait 214 215 combinations depend on trade-offs representing different ecological strategies, but at the community level trait combinations are expected to be decoupled from these trade-offs 216 because different strategies can facilitate co-existence within communities. A key remaining 217 question is to what extent community-level trait composition is globally filtered and how well 218 it is related to global vs. local environmental drivers. Here, we perform a global, plot-level 219 analysis of trait-environment relationships, using a database with more than 1.1 million 220 221 vegetation plots and 26,632 plant species with trait information. Although we found a strong filtering of 17 functional traits, similar climate and soil conditions support communities 222 differing greatly in mean trait values. The two main community trait axes which capture half 223 224 of the global trait variation (plant stature and resource acquisitiveness) reflect the trade-offs at the species level but are weakly associated with climate and soil conditions at the global scale. 225 226 Similarly, within-plot trait variation does not vary systematically with macro-environment. Our results indicate that, at fine spatial grain, macro-environmental drivers are much less 227 important for functional trait composition than has been assumed from floristic analyses 228 229 restricted to co-occurrence in large grid cells. Instead, trait combinations seem to be predominantly filtered by local-scale factors such as disturbance, fine-scale soil conditions, 230 231 niche partitioning or biotic interactions.

232

233 Introduction

How climate drives the functional characteristics of vegetation across the globe has been a 234 key question in ecological research for more than a century¹. While functional information is 235 available for a large portion of the global pool of plant species, we do not know how 236 functional traits of the different species that co-occur in a community are combined, which is 237 what determines their joint effect on ecosystems²⁻⁴. At the species level, Díaz et al.⁵ 238 demonstrated that 74% of the global spectrum of six key plant traits determining plant fitness 239 in terms of survival, growth and reproduction can be accounted for by two principal 240 241 components (PCs). They showed that the functional space occupied by vascular plant species is strongly constrained by trade-offs between traits and converges on a small set of successful 242 trait combinations, confirming previous findings⁶⁻⁹. While these constraints describe 243 evolutionarily viable ecological strategies for vascular plant species globally, they provide 244 only limited insight into trait composition within communities. There are many reasons why 245 trait composition within communities would produce very different patterns, and indeed much 246 theory predicts this¹⁰⁻¹¹. However, it is still unknown to what extent community-level trait 247 composition depends on local factors (microclimate, fine-scale soil properties, disturbance 248 regime¹⁰, successional dynamics²) and regional to global environmental drivers 249 (macroclimate^{6,12-13}, coarse-scale soil properties^{3,14}). As ecosystem functions and services are 250 ultimately dependent on the traits of the species composing ecological communities. 251 252 exploring community trait composition at the global scale can advance our understanding of how climate change and other anthropogenic drivers affect ecosystem functioning. 253

So far, studies relating trait composition to the environment at continental to global extents 254 have been restricted to coarse-grained species occurrence data (e.g. presence in 1° grid cells¹⁵⁻ 255 ¹⁷). Such data capture neither biotic interactions (co-occurrence in large grid cells does not 256 indicate local co-existence), nor local variation in environmental filters (e.g. variation in soil, 257 topography or disturbance regime within grid cells). In contrast, functional composition of 258 ecological communities sampled at fine-grained vegetation plots - with areas of few to a few 259 hundred square meters – is the direct outcome of the interaction between both local and large-260 scale factors. Here, we present a global analysis of plot-level trait composition. We combined 261 262 the 'sPlot' database, a new global initiative incorporating more than 1.1 million vegetation plots from over 100 databases (mainly forests and grasslands; see Methods), with 30 large-263 scale environmental variables and 18 key plant functional traits derived from TRY, a global 264 265 plant-trait database (see Methods, Table 2). We selected these 18 traits because they affect different key ecosystem processes and are expected to respond to macroclimatic drivers 266 (Table 1). In addition, they were sufficiently measured across all species globally to allow for 267 imputation of missing values (see Methods). All analyses were confined to vascular plant 268 species and included all vegetation layers in a community, from the canopy to the herb layer 269 270 (see Methods).

We used this unprecedented fine-resolution dataset to test the hypothesis (Hypothesis 1) that 271 272 plant communities show evidence of environmental or biotic filtering at the global scale, making use of the observed variation of plot-level trait means and means of within-plot trait 273 274 variation across communities. Ecological theory suggests that community-level convergence could be interpreted as the result of filtering processes, including environmental filtering and 275 276 biotic interactions. Globally, temperature and precipitation drive the differences in vegetation between biomes, suggesting strong environmental filtering^{3,11} that constrains the number of 277 successful trait combinations and leads to community-level trait convergence. Similarly, 278 biotic interactions may eliminate excessively divergent trait combinations^{18,19}. However, 279 alternative functional trait combinations may confer equal fitness in the same environment¹⁰. 280 If plant communities show a global variation of plot-level trait means higher than expected by 281 282 chance, and a lower than expected within-plot trait variation (see Figure 1), this would support the view that environmental or biotic filtering are dominant structuring processes of 283 community trait composition at the global scale. A consequence of strong community-level 284 trait convergence, and thus low variation within plots with species trait values centred around 285 the mean, would be that plot-level means will be similar to the trait values of the species in 286 that plot. Hence, community mean trait values should then mirror the trait values of individual 287 species⁵. 288

289 While Hypothesis 1 addresses the degree of filtering, it does not make a statement on the attribution of driving factors. The main drivers should correlate strongly (though not 290 necessarily linearly²⁰) with plot-level trait means and within-plot trait variance. Identifying 291 these drivers has the potential to fundamentally improve our understanding of global trait-292 293 environment relationships. We tested the hypothesis (Hypothesis 2) that there are strong correlations between global environmental drivers such as macroclimate and coarse-scale soil 294 properties and both plot-level trait means and within-plot trait variances^{3,6,12-17,20-24} (see Table 295 1 for expected relationships and Supplementary Table 2 for variables used). Such evidence, 296

although correlative, may contribute to the formulation of novel hypotheses to explain globalplant trait patterns.

299

300 Results and Discussion

301 Consistent with Hypothesis 1 and as illustrated in Figure 1, global variation in plot-level trait 302 means was much higher than expected by chance: all traits had positive standardized effect 303 sizes (SESs), which were significantly > 0 for 17 out of 18 traits based on gap-filled data 304 (mean SES = 8.06 standard deviations (SD), Table 2). This suggests that environmental or 305 biotic filtering is a dominant force of community trait composition globally. Also as predicted 306 by Hypothesis 1, within-plot trait variance was typically lower than expected by chance (mean SES = -1.76 SD, significantly < 0 for ten traits but significantly > 0 for three traits; 307 Table 2). Thus, trait variation within communities may also be constrained by filtering. 308

Trait correlations at the community level were relatively well captured by the first two axes of 309 a Principal Component Analysis (PCA) for both plot-level trait means and within-plot trait 310 311 variances (Figures 1 and 2). The dominant axes were determined by those traits with the 312 highest absolute SESs of plot-level trait mean trait values (Table 2, mean of CWMs). The PCA of plot-level trait means (Fig. 2) reflects two main functional continua on which 313 314 community trait values converge: one from short-stature, small-seeded communities such as grasslands or herbaceous vegetation to tall-stature communities with large, heavy diaspores 315 such as forests (the size spectrum), and the other from communities with resource-acquisitive 316 to those with resource-conservative leaves (i.e. the leaf economics spectrum)⁷. The high 317 similarity between this PCA and the one at the species level by Díaz et al.⁵ is striking: here at 318 319 the community level, based on 1.1 million plots, the same functional continua emerged as at the species level, based on 2,214 species. While the trade-offs between different traits at the 320 321 species level can be understood from a physiological and evolutionary perspective, finding 322 similar trade-offs between traits at the community level was unexpected, as species with opposing trait values can co-exist in the same community. In combination with our finding of 323 324 strong trait convergence, these results reveal a strong parallel of present-day community 325 assembly to individual species' evolutionary histories.

Surprisingly, we found only limited support for Hypothesis 2. Community-level trait 326 composition was poorly captured by global climate and soil variables. None of the 30 327 environmental variables accounted individually for more than 10% of the variance in the traits 328 defining the main dimensions in Fig. 2 (Supplementary Fig. 2). The coefficients of 329 330 determination were not improved when testing for non-linear relationships (see Methods). Using all 30 environmental variables simultaneously as predictors only accounted for 10.8% 331 or 14.0% of the overall variation in plot-level trait means (cumulative variance, respectively, 332 333 of the first two or all 18 constrained axes in a Redundancy Analysis). Overall, our results show that similar global-scale climate and soil conditions can support communities that differ 334 335 markedly in mean trait values and that different climates can support communities with rather similar mean trait values. 336

- The ordination of within-plot variance of the different traits (Fig. 3) revealed two main
- continua. Variances of plant height and diaspore mass varied largely independently of
- variances of traits representing the leaf economics spectrum. This suggests that short and tall
- 340 species can be assembled together in the same community independently from combining
- 341 species with acquisitive leaves with species with conservative leaves. Global climate and soil
- variables accounted for even less variation on the first two PCA axes in within-plot trait
- variances than on the first two PCA axes in plot-level trait means. Only two environmental variables had $r^2 > 3\%$ (Supplementary Fig. 3), whether allowing for non-linear relationships
- (see Methods) or not, and overall, macro-environment accounted for only 3.6% or 5.0% of the
- variation (cumulative variance, respectively, of the first two or all 18 constrained axes).
- 347 Removing species richness effects from within-plot trait variances did not increase the
- amount of variation explained by the environment (see Methods).
- 349 The findings of our study contrast strongly with studies where the variation in traits between species was calculated at the level of the species pool in large grid cells^{15,16}, suggesting that 350 plot-level and grid cell-level trait composition are driven by different factors²¹. Plot-level trait 351 means and variances may both be predominantly driven by local environmental factors, such 352 as topography (e.g. north-vs. south-facing slopes), local soil characteristics (e.g. soil depth 353 and nutrient supply)^{3,14,24,25}, disturbance regime (including land use²⁶ and successional 354 status^{2,27}) or biotic interactions^{18-19,28}, while broad-scale climate and soil conditions may only 355 become relevant for the whole species pool in large grid cells. Such differences emphasize the 356 357 importance of local environment in affecting the communities' trait composition and should be taken into account when interpreting the effect of environmental drivers in functional trait 358 359 diversity using data on either floristic pools or ecological communities.
- We note that the strongest community-level correlations with environment were found for 360 traits not linked to the leaf economics spectrum. Mean stem specific density increased with 361 potential evapotranspiration (PET, $r^2=15.6\%$; Fig. 4a, b), reflecting the need to produce 362 denser wood with increasing evaporative demand. Leaf N:P ratio increased with growing-363 season warmth (growing degree days above 5°C, GDD5, $r^2=11.5\%$; Fig. 4d), indicating strong 364 phosphorus limitation²⁹ in most plots in the tropics and subtropics (Fig. 4c, d). This pattern 365 was not brought about by a parallel increase in the presence of legumes, which tend to have 366 367 relatively high N:P ratios; excluding all species of Fabaceae resulted in a very similar relationship with GDD5 ($r^2=10.0\%$). The global N:P pattern is consistent with results based 368 on traits of single species related to mean annual temperature 30 . We assume that the main 369 underlying mechanism is the high soil weathering rate at high temperatures and humidity, 370 371 which in the tropics and subtropics was not reset by Pleistocene glaciation. Thus, phosphorus 372 limitation may weaken the relationships between productivity-related traits and macroclimate (Supplementary Fig. 2). For example, specific leaf area may be low as consequence of low 373 nutrient availability^{3,14,24-25} in favourable climates as well as be low as consequence of low 374 temperature and precipitation under favourable nutrient supply. Overall, our findings are 375 relevant in improving Dynamic Global Vegetation Models (DGVMs), which so far have used 376 trait information only from a few calibration plots²². The sPlot database provides much-377 needed empirical data on the community trait pool in DGVMs³¹ and identifies traits that 378

should be considered when predicting ecosystem functions from vegetation, such as stemspecific density and leaf N:P ratio.

381 Our results were surprisingly robust both to the selection of trait data, when comparing 382 different plant formations and when explicitly accounting for the uneven distribution of plots. 383 Using the original trait values measured for the species from the TRY database for the six traits used by Díaz et al.⁵ (see Methods), resulted in the same two main functional continua 384 and an overall highly similar ordination pattern (Supplementary Fig. 4) compared to using 385 gap-filled data for 18 traits (Fig. 2). Community-level trait composition was also similarly 386 387 poorly captured by global climate and soil variables. Single regressions of CWMs with all 388 environmental variables revealed very similar patterns to those based on gap-filled traits (Supplementary Fig. 5). Similarly, subjecting the CWMs based on six original traits to a 389 Redundancy Analysis with all 30 environmental variables accounted only for 20.6% or 21.8% 390 391 of the overall variation in CWMs (cumulative variance of the first two or all six constrained axes, respectively, Supplementary Fig. 4). These results clearly demonstrate that the 392 393 imputation of missing trait values did not result in spurious artefacts which may have 394 obscured community trait-environment relationships.

395 We also assessed whether the observed trait-environment relationships hold for forests and non-forest vegetation independently (see Methods). Both subsets confirmed the overall 396 patterns in trait means (Supplementary Figs. 3-6). The variance in plot-level trait means 397 explained by large-scale climate and soil variables was higher for forest than non-forest plots, 398 probably because forests belong to a well-defined and rather resource-conservative formation, 399 400 whereas non-forest plots encompass a heterogeneous mixture of different vegetation types, ranging from alpine meadows to semi-deserts, and tend to depend more on disturbance and 401 management, which can strongly affect trait-environment relationships of communities²¹. 402 403 Finally, to test whether our findings depended on the uneven distribution of plots among the world's different climates and soils, we repeated the analyses in 100 subsets of ~100,000 plots 404 405 resampled in the global climate space (Supplementary Figs. 7-8). The analyses of the 406 resampled datasets revealed the same patterns and confirmed the impact of PET and GDD5 407 on stem specific density and leaf N:P ratio, respectively. The correlations between trait means and environmental variables were, however, stronger in the resampled subsets, possibly 408 409 because the resampling procedure reduced the overrepresentation of the temperate-zone areas 410 with intermediate climatic values.

Our findings have important implications for understanding and predicting plant community 411 trait assembly. First, worldwide trait variation of plant communities is captured by a few main 412 dimensions of variation, which are surprisingly similar to those reported by species-based 413 studies^{5,7-9}, suggesting that the drivers of past trait evolution, which resulted in the present-day 414 species-level trait spectra⁵, are also reflected in the composition of today's plant communities. 415 If species-level trade-offs indeed constrain community assembly, then the present-day 416 417 contrasts in trait composition of terrestrial plant communities should also have existed in the past and will probably remain, even for novel communities, in the future. Most species in our 418 present-day communities evolved under very variable filtering conditions across the globe, 419 with respect to temperature and precipitation regimes. Therefore, it can be assumed that future 420 filtering conditions will result in novel communities that follow the same functional continua 421

from short-stature, small-seeded communities to tall-stature communities with large, heavy 422 423 diaspores and from communities with resource-acquisitive to those with resourceconservative leaves. Second, the main plot-level vegetation trait continua cannot easily be 424 captured by coarse-resolution environmental variables²¹. This brings into question both the 425 use of simple large-scale climate relationships to predict the leaf economics spectra of global 426 vegetation^{13,15-16,22} and attempts to derive net primary productivity and global carbon and 427 water budgets from global climate, even when employing powerful trait-based vegetation 428 models³¹. The finding that within-plot trait variances were only very weakly related to global 429 climate or soil variables points to the importance of i) local-scale climate or soil variables, ii) 430 disturbance regimes or iii) biotic interactions for the degree of local trait dispersion¹¹. Finally, 431 both our findings on the limited role of large-scale climate in explaining trait patterns and on 432 the prevalence of phosphorus limitation in most plots in the tropics and subtropics call for 433 including local variables when predicting community trait patterns. Even under similar 434 macro-environmental conditions, communities can vary greatly in trait means and variances, 435 consistent with high local variation in species' trait values^{3,6-7}. Future research on functional 436 response of communities to changing climate should incorporate the effect of local 437 environmental conditions²⁴⁻²⁶ and biotic interactions¹⁸⁻¹⁹ for building reliable predictions of 438 vegetation dynamics. 439

440

441 Material and Methods

Vegetation Data. The sPlot 2.1 vegetation database contains 1,121,244 plots with 23,586,216
species × plot observations, i.e. records of a species in a plot

444 (https://www.idiv.de/en/sdiv/working_groups/wg_pool/splot.html). This database aims at

445 compiling plot-based vegetation data from all vegetation types worldwide, but with a

446 particular focus on forest and grassland vegetation. Although the initial aim of sPlot was to

447 achieve global coverage, the plots are very unevenly distributed with most data coming from

- Europe, North America and Australia and an overrepresentation of temperate vegetation types
- 449 (Supplementary Fig. 1).

450 For most plots (97.2%) information on the single species' relative contribution to the sum of plants in the plot was available, expressed as cover, basal area, individual count, importance 451 value or per cent frequency in subplots. For the other 2.8% (31,461 plots), for which only 452 presence/absence (p/a) was available, we assigned equal relative abundance to the species 453 (1/species richness). For plots with a mix of cover and p/a information (mostly forest plots, 454 455 where herb layer information had been added on a p/a basis; 8,524 plots), relative abundance 456 was calculated by assigning the smallest cover value that occurred in a particular plot to all species with only p/a information in that plot. In most cases (98.4%), plot records in sPlot 457 include full species lists of vascular plants. Bryophytes and lichens were additionally 458 identified in 14% and 7% of plots, respectively. After removing plots without geographic 459 460 coordinates and all observations on bryophytes and lichens, the database contained 22,195,966 observations on the relative abundance of vascular plant species in a total of 461 462 1,117,369 plots. The temporal extent of the data spans from 1885 to 2015, but >95% of 463 vegetation plots were recorded later than 1980. Plot size was reported in 65.4% of plots.

- 464 While forest plots had plot sizes $\ge 100 \text{ m}^2$, and in most cases $\le 1,000 \text{ m}^2$, non-forest plots 465 typically ranged from 5 to 100 m².
- **Taxonomy.** To standardize the nomenclature of species within and between sPlot and TRY
- 467 (see below), we constructed a taxonomic backbone of the 121,861 names contained in the two
- 468 databases. Prior to name matching, we ran a series of string manipulation routines in R, to
- remove special characters and numbers, as well as standardized abbreviations in names.
- 470 Taxon names were parsed and resolved using Taxonomic Name Resolution Service version
- 471 4.0 (TNRS³²; <u>http://tnrs.iplantcollaborative.org</u>; accessed 20 Sep 2015), selecting the best
- 472 match across the five following sources: i) The Plant List (version 1.1;
- 473 http://www.theplantlist.org/; Accessed 19 Aug 2015), ii) Global Compositae Checklist (GCC,
- 474 <u>http://compositae.landcareresearch.co.nz/Default.aspx;</u> accessed 21 Aug 2015), iii)
- 475 International Legume Database and Information Service (ILDIS,
- 476 <u>http://www.ildis.org/LegumeWeb;</u> accessed 21 Aug 2015), iv) Tropicos
- 477 (http://www.tropicos.org/; accessed 19 Dec 2014), and v) USDA Plants Database
- 478 (http://usda.gov/wps/portal/usda/usdahome; accessed 17 Jan 2015). We allowed for partial
- 479 matching to the next higher taxonomic rank (genus or family) in cases where full taxon names
- 480 could not be found. All names matched or converted from a synonym by TNRS were
- 481 considered accepted taxon names. In cases when no exact match was found (e.g. when
- 482 alternative spelling corrections were reported), names with probabilities of \geq 95% or higher
- 483 were accepted and those with < 95% were examined individually. Remaining non-matching
- anames were resolved based on the National Center for Biotechnology Information's
- 485 Taxonomy database (NCBI, <u>http://www.ncbi.nlm.nih.gov/;</u> accessed 25 Oct 2011) within
- 486 TNRS, or sequentially compared directly against The Plant List and Tropicos (accessed
- 487 September 2015). Names that could not be resolved against any of these lists were left as
- blanks in the final standardized name field. This resulted in a total of 86,760 resolved names,
- 489 corresponding to 664 families, occurring in sPlot or TRY or both. Classification into families
- 490 was carried out according to $APGIII^{33}$, and was used to identify non-vascular plant species
- 491 (\sim 5.1% of the taxon names) which were excluded from the subsequent statistical analysis.
- 492 **Trait Data.** Data for 18 traits that are ecologically relevant (Table 1) and sufficiently covered 493 across species³⁴ were requested from TRY^{35} (version 3.0) on the 10th August, 2016. We
- 494 applied gap-filling with Bayesian Hierarchical Probabilistic Matrix Factorization
- (BHPMF $^{34,36-37}$). We used the prediction uncertainties provided by BHPMF for each
- 496 imputation to assess the quality of gap-filling and removed all imputations with a coefficient 1^{37} where 1^{37} we have 1^{37} with a set of 1^{3
- 497 of variation $> 1^{37}$. We obtained 18 gap-filled traits for 26,632 out of a total of 58,065 taxa in
- sPlot, which corresponds to 45.9% of all species but to 88.7% of all species × plot
 combinations. Trait coverage of the most frequent species was 77.2% and 96.2% for taxa that
- 500 occurred in more than 100 or 1,000 plots, respectively. The gap-filled trait data comprised
- 501 observed and imputed values on 632,938 individual plants, which we log_e transformed and
- aggregated by taxon. For those taxa that were recorded at the genus level only, we calculated
- 503 genus means. Out of 22,195,966 records of vascular plant species with geographic reference,
- 21,172,989 (=95.4%) refer to taxa for which we had gap-filled trait values. This resulted in
- 505 1.115.785 and 1.099.463 plots for which we had at least one taxon or two taxa with a trait

value (99.5% and 98.1%, respectively, of all 1,121,244 plots), and for which trait means and
variances could be calculated.

As some mean values of traits in TRY were based on a very small number of replicates per species, which results in uncertainty in trait mean and variance calculations³⁸, we tested to which degree the trait patterns in the dataset might be caused by a potential removal of trait variation by imputation of trait values and additionally carried out all analyses using the

- 512 original trait data on the same 632,938 individual plants instead of gap-filled data
- 513 (Supplementary Table 1). The degree of trait coverage of species ranged between 7.0% and
- 514 58.0% for leaf fresh mass and plant height, respectively. Across all species, mean coverage of
- species with original trait values was 21.8%, as compared to 45.9% for gap-filled trait data.
- 516 Linking these trait values to the species occurrence data resulted in a coverage of species ×
- 517 plot observations with trait values between 7.6% and 96.6% for conduit element length and
- plant height, respectively (Supplementary Table 1), with a mean of 60.7% as compared to
- 51988.7% for those based on gap-filled traits. Using these original trait values to calculate
- community-weighted mean (CWM) trait values (see below) resulted in a plot coverage of trait
- values between 48.2% and 100% for conduit element length and SLA, respectively. Across all
- plots, mean coverage of plots with original trait values was 89.3%, as compared to 100% for
- 523 gap-filled trait data (Supplementary Table 1).
- 524 We are aware that using species mean values for traits excludes the possibility to account for $\frac{39}{70}$ min
- 525 intraspecific variance, which can also strongly respond to the environment³⁹. Thus, using one
- single value for a species is a source of error in calculating trait means and variances.
- 527
- **Environmental Data.** We compiled 30 environmental variables (Supplementary Table 2).
- 529 Macroclimate variables were extracted from CHELSA⁴⁰⁻⁴¹, V1.1 (Climatologies at High
- 530 Resolution for the Earth's Land Surface Areas, <u>www.chelsa-climate.org</u>). CHELSA provides
- 19 bioclimatic variables equivalent to those used in WorldClim (<u>www.worldclim.org</u>) at a
- resolution of 30 arc sec (\sim 1 km at the equator), averaging global climatic data from the
- period 1979–2013 and using a quasi-mechanistic statistical downscaling of the ERA-Interim
 reanalysis⁴².
- 535 Variables reflecting growing-season warmth were growing degree days above $1^{\circ}C$ (GDD1)
- and $5^{\circ}C$ (GDD5), calculated from CHELSA data⁴³. We also compiled an index of aridity
- 537 (AR) and a model for potential evapotranspiration (PET) extracted from the Consortium of
- 538 Spatial Information (CGIAR-CSI) website (<u>www.cgiar-csi.org</u>). In addition, seven soil
- variables were extracted from the SOILGRIDS project (<u>https://soilgrids.org/</u>, licensed by
- 540 ISRIC World Soil Information), downloaded at 250 m resolution and then resampled using
- the 30 arc second grid of CHELSA (Supplementary Table 2). We refer to these climate and
- 542 soil data as "environmental data".

543 **Community trait composition.**

For every trait *j* and plot *k*, we calculated the plot-level trait means as community-weighted mean (CWM) according to^{2,44}:

$$CWM_{j,k} = \sum_{i}^{n_k} p_{i,k} t_{i,j}$$

where n_k is the number of species sampled in plot k, $p_{i,k}$ is the relative abundance of species iin plot k, referring to the sum of abundances for all species with traits in the plot, and $t_{i,j}$ is the mean value of species i for trait j. This computation was done for each of the 18 traits for 1,115,785 plots. The within-plot trait variance is given by community-weighted variance (CWV)^{44,45}:

$$CWV_{j,k} = \sum_{i}^{n_k} p_{i,k} (t_{i,j} - CWM_{j,k})^2$$

551 CWV is equal to functional dispersion as described by Rao's quadratic entropy⁴⁶, when using 552 a squared Euclidean distance matrix $d_{i,i,k}$ ⁴⁷:

$$CWV_{j,k} = \sum_{i}^{n_k} p_{i,k} (t_{i,j} - CWM_{j,k})^2 = FD_Q = \sum_{i=1}^{n_k-1} \sum_{j=i+1}^{n_k} p_{i,k} p_{j,k} d_{i,j,k}^2$$

We had CWV information for 18 traits for 1,099,463 plots, as at least two taxa were needed to calculate CWV. We performed the calculations using the 'data.table' package⁴⁸ in R.

555

Assessing the degree of filtering. To analyse how plot-level trait means and within-plot trait 556 557 variances (based on gap-filled trait data) depart from random expectation, for each trait we 558 calculated standardized effect sizes (SESs) for the variance in CWMs and for the mean in 559 CWVs. Significantly positive SESs in variance of CWM and significantly negative ones in 560 the mean of CWV can be considered a global-level measure of environmental or biotic 561 filtering. To provide an indication of the global direction of filtering, we also report SESs for the mean of CWM trait values. Similarly, to measure how much within-community trait 562 563 dispersion varied globally, we also calculated SESs for the variance in CWV. SESs were obtained from 100 runs of randomizing trait values across all species globally. In 564

every run we calculated CWM and CWV with random trait values, but keeping all species 565 abundances in plots. Thus, the results of randomization are independent from species co-566 occurrences structure of plots⁴⁹. For every trait, the SESs of the variance in CWM were 567 calculated as the observed value of variance in CWM minus the mean variance in CWM of 568 569 the random runs, divided by the standard deviation of the variance in CWM of the random runs (Fig. 1). SESs for the mean in CWM, the mean in CWV and the variance in CWV were 570 calculated accordingly. Tests for significance of SESs were obtained by fitting generalized 571 Pareto-distribution of the most extreme random values and then estimating p values form this 572 573 fitted distribution⁵⁰.

574

575 Vegetation trait-environment relationships. Out of the 1,115,785 plots with CWM values,
576 1,114,304 (99.9%) had complete environmental information and coordinates. This set of plots

- was used to calculate single linear regressions of each of the 18 traits on each of the 30
 environmental variables. We used the 'corrplot' function⁵¹ in R to illustrate Pearson
- 579 correlation coefficients (see Supplementary Figs. 1-2, 4, 6, 8) and for the strongest
- relationships produced bivariate graphs and mapped the global distribution of the CWM
- values using kriging interpolation in ArcGIS 10.2 (Fig. 4). We also tested for non-linear
- relationships with environment by including an additional quadratic term in the linear model
- and then report coefficients of determination. As in the linear relationships of CWM with
- environment, the highest r^2 values in models with an additional quadratic term were
- encountered between stem specific density and PET ($r^2=0.156$) and leaf N:P ratio and
- growing degree days above 5°C (GDD5, $r^2=0.118$). These were not substantially different
- from the linear CWM-environment relationships, which had $r^2=0.156$ and $r^2=0.115$,
- respectively (Fig. 4, Supplementary Fig. 2). Similarly, including a quadratic term in the
- regressions did not increase the CWV-environment correlations. Here, the strongest
- correlations were encountered between plant height and soil pH ($r^2=0.044$) and between
- specific leaf area (SLA) and the volumetric content of coarse fragments in the soil
- 592 (CoarseFrags, $r^2=0.037$), which were similar to those in the linear regressions ($r^2=0.029$ and
- 593 $r^2=0.036$, respectively, Supplementary Fig. 3).
- To account for a possible confounding effect of species richness on CWV, which may cause low CWV through competitive exclusion of species, we regressed CWV on species richness and then calculated all Pearson correlation coefficients with the residuals of this relationship
- and then calculated an Pearson correlation coefficients with the residuals of this relationshipagainst all climatic variables. Here, the highest correlation coefficients were encountered
- between PET and CWV of conduit element length (r^2 =0.038), followed by the relationship of
- specific leaf area (SLA) and the volumetric content of coarse fragments in the soil
- 600 (CoarseFrags, $r^2=0.034$), which were very similar in magnitude to the CWV environment
- (Coarseriags, 1 0.054), which were very similar in magnitude to the C w V environme correlations ($r^2=0.025$ and $r^2=0.026$, respectively. Supplementary Fig. 2)
- 601 correlations ($r^2=0.035$ and $r^2=0.036$, respectively; Supplementary Fig. 3).
- The CWMs and CWVs were scaled to a mean of zero and standard deviation of one and then subjected to a Principal Component Analysis (PCA), calculated with the 'rda' function from the 'vegan' package⁵². Climate and soil variables were fitted *post hoc* to the ordination scores of plots of the first two axes, producing correlation vectors using the 'envfit' function. We refrain from presenting any inference statistics, as with > 1.1 million plots all environmental
- variables showed statistically significant correlations. Instead, we report coefficients of
- determination (r^2) , obtained from Redundancy Analysis (RDA), using all 30 environmental
- variables as constraining matrix, resulting in a maximum of 18 constrained axes
- 610 corresponding to the 18 traits. We report both r^2 values of the first two axes explained by
- 611 environment, which is the maximum correlation of the best linear combination of
- environmental variables to explain the CWM or CWV plot \times trait matrix and r² values of all
- 613 18 constrained axes explained by environment. We plotted the PCA results using the 'ordiplot'
- function and coloured the points according to the logarithm of the number of plots that fell
- 615 into grid cells of 0.002 in PCA units (resulting in approximately 100,000 cells). For further
- 616 details, see the captions of the figures.
- Additionally, we carried out the PCA and RDA analyses, using CWMs based on original trait
- values (see above). Because of a poor coverage of some traits we confined the analyses with
- original trait values to the six traits used by Díaz et al. 5 , which were leaf area, specific leaf

area, leaf N, seed mass, plant height and stem specific density. Using these six traits resulted

621 in 954,459 plots that had at least one species with a trait value for each of the six traits.

622

623 Testing for formation-specific patterns. We carried out separate analyses for two 'formations': forest and for non-forest plots. We defined as forest plots that had > 25% cover 624 of the tree layer. However, this information was available for only 25% of the plots in our 625 sPlot database. Thus, we also assigned formation status based on growth form data from the 626 627 TRY database. We defined plots as 'forest' if the sum of relative cover of all tree taxa was > 25%, but only if this did not contradict the requirement of > 25% cover of the tree layer (for 628 629 those records for which this information was given in the header file). Similarly, we defined 630 non-forest plots by calculating the cover of all taxa that were not defined as trees and shrubs (also taken from the TRY plant growth form information) and that were not taller than 2 m, 631 using the TRY data on mean plant height. We assigned the status 'non-forest' to all plots that 632 had >90% cover of these low-stature, non-tree and non-shrub taxa. In total, 21,888 taxa out of 633 the 52,032 in TRY which also occurred in sPlot belonged to this category, and 16,244 were 634 classed as trees. The forests and non-forest plots comprised 330,873 (29.7%) and 513,035 635 (46.0%) of all plots, respectively. We subjected all CWM values for forest and non-forest 636 plots to PCA, RDA and bivariate linear regressions to environmental variables as described 637 above. 638

The forest plots, in particular, confirmed the overall patterns, with respect to variation in 639 CWM explained by the first two PCA axes (60.5%) and the two orthogonal continua from 640 641 small to large size and the leaf economics spectrum (Supplementary Fig. 6). The variation explained by macroclimate and soil conditions was much larger for the forest subset than for 642 the total data, with the best relationship (leaf N:P ratio and the mean temperature of the 643 coldest quarter, bio11) having $r^2=0.369$ and the second next best ones (leaf N:P ratio and 644 GDD1 and GDD5) close to this value with $r^2=0.357$ (Supplementary Fig. 7) and an overall 645 variation in CWM values explained by environment of 25.3% (cumulative variance of all 18 646 647 constrained axes in a RDA). The non-forest plots showed the same functional continua, but with lower total amount of variation in CWM accounted for by the first two PCA axes 648 (41.8%, Supplementary Fig. 8) and much lower overall variation explained by environment. 649 650 For non-forests, the best correlation of any CWM trait with environment was the one of 651 volumetric content of coarse fragments in the soil (CoarseFrags) and leaf C content per dry mass with $r^2=0.042$ (Supplementary Fig. 9). Similarly, the cumulative variance of all 18 652 constrained axes according to RDA was only 4.6%. This shows, on the one hand, that forest 653 654 and non-forest vegetation are characterized by the same interrelationships of CWM traits, and on the other hand, that the relationships of CWM values with the environment were much 655 stronger for forests than for non-forest formations. The coefficients of determination were 656 even higher than those previously reported for trait-environment relationships for North 657 American forests (between CWM of seed mass and maximum temperature, $r^2=0.281$)³. 658

Resampling procedure in environmental space. In order to achieve a more even representation of plots across the global climate space, we first subjected the same 30 global climate and soil variables as described above, to a Principal Component Analysis (PCA),

using the climate space of the whole globe, irrespective of the presence of plots in this space, 662 663 and scaling each variable to a mean of zero and a standard deviation of one. We used a 2.5 arc 664 minute spatial grid, which comprised 8,384,404 terrestrial grid cells. We then counted the number of vegetation plots in the sPlot database that fell into each grid cell. For this analysis, 665 we did not use the full set of 1,117,369 plots with trait information (see above), but only those 666 plots that had a location inaccuracy of max. 3 km, resulting in a total of 799,400 plots. The 667 resulting PCA scores based on the first two principal components (PC1-PC2) were rasterized 668 to a 100×100 grid in PC1-PC2 environmental space, which was the most appropriate 669 670 resolution according to a sensitivity analysis. This sensitivity analysis tested different grid 671 resolutions, from a coarse-resolution bivariate space of 100 grid cells (10×10) to a very fineresolution space of 250,000 grid cells (500×500), iteratively increasing the number of cells 672 along each principal component by 10 cells. For each iteration, we computed the total number 673 of sPlot plots per environmental grid cell and plotted the median sampling effort (number of 674 plots) across all grid cells versus the resolution of the PC1-PC2 space. We found that the 675 676 curve flattens off at a bivariate environmental space of 100×100 grid cells, which was the resolution for which the median sampling effort stabilized at around 50 plots per grid cell. As 677 a result, we resampled plots only in environmental cells with more than 50 plots (858 cells in 678 679 total).

680 To optimize our resampling procedure within each grid cell, we used the heterogeneityconstrained random (HCR) resampling approach⁵³. The HCR approach selects the subset of 681 vegetation plots for which those plots are the most dissimilar in their species composition 682 683 while avoiding selection of plots representing peculiar and rare communities that differ 684 markedly from the main set of plant communities (outliers), thus providing a representative 685 subset of plots from the resampled grid cell. We used the turnover component of the Jaccard's dissimilarity index (β_{itu}^{54}) as a measure of dissimilarity. The β_{jtu} index accounts for species 686 replacement without being influenced by differences in species richness. Thus, it reduces the 687 688 effects of any imbalances that may exist between different plots due to species richness. We 689 applied the HCR approach within a given grid cell by running 1,000 iterations of randomly 690 selecting 50 plots out of the total number of plots available within that grid cell. Where the 691 cell contained 50 or fewer plots, all were included and the resampling procedure was not run. 692 This procedure thinned out over-sampled climate types, while retaining the full environmental 693 gradient.

694 All 1,000 random draws of a given grid cell were subsequently sorted according to the decreasing mean of β_{itu} between pairs of vegetation plots and then sorted again according to 695 the increasing variance in β_{itu} between pairs of vegetation plots. Ranks from both sortings 696 697 were summed for each random draw, and the random draw with the lowest summed rank was 698 considered as the most representative of the focal grid cell. Because of the randomized nature of the HCR approach, this resampling procedure was repeated 100 times for each of the 858 699 700 grid cells. This enabled us to produce 100 different subsamples out of the full sample of 701 799,400 vegetation plots subjected to the resampling procedure. Each of these 100 subsamples was finally subjected to ordinary linear regression, PCA and RDA as described 702 703 above. We calculated the mean correlation coefficient across the 100 resampled data sets for 704 each environmental variable with each trait.

- To plot bivariate relationships, we used the mean intercept and slope of these relationships. 705
- 706 PCA loadings of all 100 runs were stored and averaged. As different runs showed different
- orientation on the first PCA axes, we switched the signs of the axis loadings in some of the 707
- runs to make the 100 PCAs comparable to the reference PCA, based on the total data set. 708
- 709 Across the 100 resampled data sets, we then calculated the minimum and maximum loading
- for each of the two PCA axes and plotted the result as ellipsoid. We also collected the post-710
- hoc regressions coefficients of PCA scores with the environmental variables in each of the 711
- 100 runs, switched the signs accordingly and plotted the correlations to PC1 and PC2 as 712
- ellipsoids. The result is a synthetic PCA of all 100 runs. To illustrate the coverage of plots in 713
- PCA space, we used plot scores of one of the 100 random runs. Similarly, the coefficients of 714
- determination obtained from the RDAs of these 100 resampled sets were averaged. 715
- The mean PCA loadings across these 100 subsets (summarized in Supplementary Fig. 10) 716
- 717 were fully consistent with those of the full data set in Fig. 2, with the same two functional
- continua in plant size and diaspore mass (from bottom left to top right), and perpendicular to 718
- that, the leaf economics spectrum. The variation in CWM accounted for by the first two axes 719
- 720 was on average $50.9\% \pm 0.04$ standard deviations (SD), and thus, virtually identical with that
- in the total dataset. In contrast, the variation explained on average by macroclimate and soil 721 conditions (26.5% \pm 0.01 SD as average cumulative variance of all 18 constrained axes in the 722
- 723 RDAs across all 100 runs) was considerably larger than that for the total dataset, which is also
- 724 reflected in consistently higher correlations between traits and environmental variables
- (Supplementary Fig. 11). The highest mean correlation was encountered for plant height and 725
- PET (mean $r^2=0.342$ across 100 runs). PET was a better predictor for plant height than the 726
- precipitation of the wettest months (bio13, mean $r^2=0.231$), as had been suggested 727
- previously⁶. The correlation of PET with stem specific density (mean $r^2=0.284$) and warmth 728
- of the growing season (expressed as growing degree days above the threshold 5°C, GDD5) 729
- with leaf N:P ratio (mean $r^2=0.250$) ranked among the best 12 correlations encountered out of 730
- 731 all 540 trait-environment relationships, which confirms the patterns found in the whole data
- set (compared with Fig. 4). Overall, the coefficients of determination were much closer to the 732 ones reported from other studies with a global collection of a few hundred plots (r² values
- 733 ranging from 36% to 53% based on multiple regressions of single traits with five to six
- 734 environmental drivers²²).
- 735
- 736

737 Data availability statement

- 738 The data contained in sPlot (the vegetation-plot data complemented by trait and
- 739 environmental information) are available by request, through contacting any of the sPlot
- 740 consortium members for submitting a paper proposal. The proposals should follow the
- 741 Governance and Data Property Rules of the sPlot Working Group, which are available on the
- sPlot website (www.idiv.de/sPlot). 742
- 743

744 Acknowledgements

- sPlot has been initiated by sDiv, the Synthesis Centre of the German Centre for Integrative
- 746 Biodiversity Research (iDiv) Halle-Jena-Leipzig, funded by the German Research Foundation
- 747 (FZT 118) and now is a platform of iDiv. H.B., J.De., O.Pu, U.J., B.J.-A., J.K., D.C., F.M.S.,
- 748 M.W. and C.W. appreciate direct funding through iDiv. For all further acknowledgements see
- 749 the Supplementary Information.
- 750

751 Author contributions

752 H.B. and U.J. wrote the first draft of the manuscript, with considerable input by B.J.-A. and R.F.; H.B. carried out most of the statistical analyses and produced the graphs; H.B., O.Pu. 753 and U.J. initiated sPlot as an sDiv working group and iDiv platform; J.De. compiled the plot 754 755 databases globally; J.De., S.M.H., U.J., O.Pu. and F.J. harmonized vegetation databases; J.De. and B.J.-A. coordinated the sPlot consortium; J.K. provided the trait data from TRY; F.S. 756 performed the trait data gap filling; O.Pu. produced the taxonomic backbone; B.J.-A., G.S. 757 and E. Welk compiled environmental data and produced the global maps; S.M.H. wrote the 758 759 Turboveg v3 software, which holds the sPlot database; J.L. and T.H. wrote the resampling algorithm. Many authors participated in one or more of the three sPlot workshops at iDiv 760 where the sPlot initiative was conceived and planned, and evaluation of the data and first 761 762 drafts were discussed. All other authors contributed data. All authors contributed to writing

- the manuscript.
- 764

765 **Declaration of competing interests**

- The authors declare no competing interests.
- 767

768 **References**

- 1. Warming, E. Lehrbuch der ökologischen Pflanzengeographie Eine Einführung in die
 Kenntnis der Pflanzenvereine. (Borntraeger, Berlin, 1896).
- 2. Garnier, E. *et al.* Plant functional markers capture ecosystem properties during secondary
- succession. *Ecology* **85**, 2630–2637 (2004).
- 3. Ordoñez, J.C. *et al.* A global study of relationships between leaf traits, climate and soil
 measures of nutrient fertility. *Global Ecol. Biogeogr.* 18, 137–149 (2009).
- 4. Garnier, E., Navas, M.-L. & Grigulis, K. Plant functional diversity Organism traits,
- *community structure, and ecosystem properties.* (Oxford Univ. Press, 2016).
- 5. Díaz, S. *et al.* The global spectrum of plant form and function. *Nature* **529**, 167-171 (2016).
- 6. Moles, A.T. *et al.* Global patterns in plant height. J. Ecol. **97**, 923-932 (2009).
- 779 7. Wright, I.J. et al. The worldwide leaf economics spectrum. Nature 428, 821-827 (2004).

- 8. Reich, P.B. The world–wide 'fast–slow' plant economics spectrum: a traits manifesto. *J. Ecol.* 102, 275–301 (2014).
- 9. Adler, P.B. *et al.* Functional traits explain variation in plant life history strategies. *Proc. Natl. Acad. Sci. USA* 111, 740–745 (2014).
- 10. Marks, C.O. & Lechowicz, M.J. Alternative designs and the evolution of functional
 diversity. *Am. Nat.* 167, 55–67 (2006).
- 11. Grime, J.P. Trait convergence and trait divergence in herbaceous plant communities:
- 787 Mechanisms and consequences. J. Veg. Sci. 17, 255–260 (2006).
- 12. Muscarella, R. & Uriarte, M. Do community-weighted mean functional traits reflect
 optimal strategies? *Proc. R. Soc. B.* 283, 20152434 (2016).
- 13. Swenson, N.G. & Weiser, M.D. Plant geography upon the basis of functional traits: An
- example from eastern North American trees. *Ecology* **91**, 2234–2241 (2010).
- 14. Fyllas, N.M. et al. Basin-wide variations in foliar properties of Amazonian forest:
- phylogeny, soils and climate. *Biogeosciences* **6**, 2677-2708 (2009).
- 15. Swenson, N.G. *et al.* Phylogeny and the prediction of tree functional diversity across
 novel continental settings. *Global Ecol. Biogeogr.* 26, 553–562 (2017).
- 16. Swenson, N.G. *et al.* The biogeography and filtering of woody plant functional diversity
 in North and South America. *Global Ecol. Biogeogr.* 21, 798–808 (2012).
- 17. Wright, I.J. et al. Global climatic drivers of leaf size. Science 357: 917–921 (2017).
- 18. Mayfield, M.M. & Levine, J.M. Opposing effects of competitive exclusion on the
- phylogenetic structure of communities. *Ecol. Lett.* **13**, 1085 1093 (2010).
- 19. Kraft, N.J.B. *et al.* Community assembly, coexistence and the environmental filtering
 metaphor. *Funct. Ecol.* 29, 592–599 (2015).
- 20. Barboni, D. *et al.* Relationships between plant traits and climate in the Mediterranean
 region: A pollen data analysis. *J. Veg. Sci.* 15, 635-646 (2004).
- 805 21. Borgy, B. *et al.* Plant community structure and nitrogen inputs modulate the climate signal
 806 on leaf traits. *Global Ecol. Biogeogr.* 26, 1138-1152 (2017).
- 22. van Bodegom, P.M, Douma, J.C. & Verheijen, L.M. A fully traits-based approach to
 modeling global vegetation distribution. *Proc. Natl. Acad. Sci. USA* 111, 13733–13738
 (2014).
- 23. Moles, A.T. *et al.* Which is a better predictor of plant traits: Temperature or precipitation? *J. Veg. Sci.* 25, 1167–1180 (2014).
- 812 24. Ordoñez, J.C. *et al.* Plant strategies in relation to resource supply in mesic to wet
- environments: Does theory mirror nature? *Am. Nat.* **175**, 225–239 (2010).

- 814 25. Simpson, A.J., Richardson, S.J. & Laughlin, D.C. Soil–climate interactions explain
- variation in foliar, stem, root and reproductive traits across temperate forests. *Global Ecol. Biogeogr.* 25, 964-978 (2016).
- 26. Lienin, P. & Kleyer, M. Plant leaf economics and reproductive investment are responsive
 to gradients of land use intensity. *Agric. Ecosyst. Environ.* 145, 67-76 (2011).
- 819 27. Maire, V. *et al.* Habitat filtering and niche differentiation jointly explain species relative
- abundance within grassland communities along fertility and disturbance gradients. *New Phytol.* **196**, 497–509 (2012).
- 822 28. Craine, J.M. *et al.* Global patterns of foliar nitrogen isotopes and their relationships with
- climate, mycorrhizal fungi, foliar nutrient concentrations, and nitrogen availability *New Phytol.* 183, 980–992 (2009).
- 825 29. Güsewell, S. N:P ratios in terrestrial plants: variation and functional significance. *New*826 *Phytol.* 164, 243–266 (2004).
- 30. Reich, P.B. & Oleksyn, J. Global patterns of plant leaf N and P in relation to temperature
 and latitude, *Proc. Natl. Acad. Sci. USA* 101, 11001-11006 (2004).
- 31. Scheiter, S., Langan, L. & Higgins, S.I. Next generation dynamic global vegetation
 models: learning from community ecology. *New Phytol.* **198**, 957-969 (2013).
- 32. Boyle, B. *et al.* The Taxonomic Name Resolution Service: an online tool for automated
 standardization of plant names. *BMC Bioinformatics* 14, 16 (2013).
- 33. Bremer, B. *et al.* An update of the Angiosperm Phylogeny Group classification for the
 orders and families of flowering plants: APG III. *Bot. J. Linn. Soc.* 161, 105–121 (2009).
- 34. Schrodt, F. *et al.* BHPMF a hierarchical Bayesian approach to gap-filling and trait
 prediction for macroecology and functional biogeography. *Global Ecol. Biogeogr.* 24, 1510–
 1521 (2015).
- 35. Kattge J. *et al.* TRY—a global database of plant traits. *Glob. Change Biol.* 17, 2905–2935
 (2011).
- 36. Shan, H. *et al.* Gap filling in the plant kingdom Trait prediction using hierarchical
 probabilistic matrix factorization. *Proceedings of the 29th International Conference for*
- 842 *Machine Learning (ICML 2012)* 1303–1310 (2012).
- 37. Fazayeli, F. *et al.* Uncertainty quantified matrix completion using Bayesian Hierarchical
 Matrix factorization. 13th International Conference on Machine Learning and Applications
 (ICMLA 2014) 312–317 (2014).
- 846 38. Borgy, B. *et al.* Sensitivity of community-level trait–environment relationships to data
- representativeness: A test for functional biogeography. *Global Ecol. Biogeogr.* 26, 729–739
 (2017).

- 39. Herz, K. *et al.* Drivers of intraspecific trait variation of grass and forb species in German
 meadows and pastures. *J. Veg. Sci.* 28, 705–716 (2017).
- 40. Karger, D.N. *et al.* Climatologies at high resolution for the earth's land surface areas. *Sci.*
- 852 Data 4, 170122. doi: 10.1038/sdata.2017.122 (2017)
- 41. Karger, D.N. et al. Climatologies at high resolution for the Earth land surface areas
- 854 (Version 1.1). World Data Center for Climate (WDCC) at DKRZ. <u>http://chelsa-</u>
- 855 <u>climate.org/downloads/ (2016)</u>.
- 42. Dee, D. P. *et al.* The ERA-Interim reanalysis: configuration and performance of the data assimilation system. *Q.J.R. Meteorol. Soc.* **137**, 553–597 (2011).
- 43. Synes, N.W. & Osborne, P.E. Choice of predictor variables as a source of uncertainty in
 continental-scale species distribution modelling under climate change. *Global Ecol. Biogeogr.*
- **860 20**, 904–914 (2011).
- 44. Enquist, B. *et al.* Scaling from traits to ecosystems: developing a general trait driver
- theory via integrating trait-based and metabolic scaling theories. *Adv. Ecol. Res.* 52, 249-318
 (2015).
- 45. Buzzard, V. *et al.* Re-growing a tropical dry forest: functional plant trait composition and
 community assembly during succession. *Funct. Ecol.* **30**, 1006–1013 (2016).
- 46. Rao, C.R. Diversity and dissimilarity coefficients: A unified approach. *Theor. Popul. Biol.*21, 24–43 (1982).
- 47. Champely, S. & Chessel, D. Measuring biological diversity using Euclidean metrics. *Environ. Ecol. Stat.* 9, 167-177 (2002).
- 48. Dowle, M. *et al.* data.table: Extension of Data.frame. R package version 1.9.6. (2015)
 https://CRAN.R-project.org/package=data.table
- 49. Hawkins, B.A. et al. Structural bias in aggregated species-level variables driven by
- repeated species co-occurrences: a pervasive problem in community and assemblage data. J. *Biogeogr.* 44, 1199–1211 (2017).
- 50. Knijnenburg, T.A. *et al.* Fewer permutations, more accurate P-values. *Bioinformatics* 25,
 i161–i168 (2009).
- 51. Friendly, M. Corrgrams: Exploratory displays for correlation matrices. *Am. Statistician*,
 56, 316–324 (2002).
- 52. Oksanen, J. *et al.* vegan: Community Ecology Package. R package version 2.3-3 (2016).
 https://CRAN.R-project.org/package=vegan
- 53. Lengyel, A., Chytrý, M. & Tichý, L. Heterogeneity-constrained random resampling of
- 882 phytosociological databases. J. Veg. Sci. 22, 175–183 (2011).

- 883 54. Baselga, A. The relationship between species replacement, dissimilarity derived from
- nestedness, and nestedness. *Global Ecol. Biogeogr.* **21**, 1223-1232 (2012).
- 885 55. Garnier, E. *et al.* Towards a thesaurus of plant characteristics: an ecological contribution.
- 886 *J. Ecol.* **105**, 298-309 (2017). www.top-thesaurus.org

891	Table 1: Traits used in	this study and their	function in the community.	Traits are arranged

according to the degree to which they should respond to macroclimatic drivers. $\uparrow\downarrow$ in the trait

column denotes opposing relationships, \Im in the description column denotes trade-offs. For

trait units, plot-level trait means and within-plot trait variance see Table 2.

Trait	Description	Function	Expected correlation with macroclimate
Specific leaf area, Leaf area, Leaf fresh mass, Leaf N, Leaf P ↑↓ Leaf dry matter content, Leaf N per area, Leaf C	Leaf economics spectrum ^{7-8,17} : Thin, N-rich leaves with high turnover and high mass-based assimilation rates $\widehat{\psi}$ Thick, N-conservative, long-lived leaves with low mass-based assimilation rates	Productivity, competitive ability	Very high ¹²⁻ 13,17,21,23
Stem specific density	Fast growth ≎ Mechanical support, Longevity	Productivity, drought tolerance	Very high ^{12,22}
Conduit element length ↑↓ Stem conduit density	Efficient water transport û Safe water transport	Water use efficiency	High
Plant height	Mean individual height of adult plants	Competitive ability	High ^{6,12}
Seed number per reproductive unit ↑↓ Seed mass, Seed length, Dispersal unit length	Seed economics spectrum ²³ : Small, well dispersed seeds Seeds with storage reserve to facilitate establishment and increase survival	Dispersal, regeneration	Moderate ²³⁻²⁴
Leaf N:P ratio	P limitation (N:P > 15) N limitation (N:P < 10) ²⁹	Nutrient supply	Moderate ³⁰
Leaf nitrogen isotope ratio (leaf $\delta^{15} \text{N})$	Access to N derived from N ₂ fixation N supply via mycorrhiza	Nitrogen source, soil depth	Moderate ²⁸

895

Table 2: Traits, abbreviation of trait names, identifier in the Thesaurus Of Plant characteristics (TOP)⁵⁵, units of measurement, observed values 897 (obs.) standardized effect sizes (SES) and significance (p) of SES for means and variances of both plot-level trait means (community-weighted 898 means, CWMs) and within-plot trait variances (community-weighted variances, CWVs). CWMs and CWVs were based on gap-filled traits for 899 1,115,785 and 1,099,463 plots, respectively. All trait values were loge-transformed prior to analysis and observed values are on the loge scale. SES 900 are also based on log_e-transformed values. Stem specific density is stem dry mass per stem fresh volume, specific leaf area is leaf area per leaf dry 901 mass, leaf C, N and P are leaf carbon, nitrogen and phosphorus content, respectively, per leaf dry mass, leaf dry matter content is leaf dry mass per 902 leaf fresh mass, leaf delta ¹⁵N is the leaf nitrogen isotope ratio, stem conduit density is the number of vessels and tracheids per unit area in a cross 903 section, conduit element length refers to both vessels and tracheids. SESs were calculated by randomizing trait values across all species globally 100 904 times and calculating CWM and CWV with random trait values, but keeping all species abundances in plots (see Fig. 1). Tests for significance of 905 SES were obtained by fitting generalized Pareto-distribution of the most extreme random values and then estimating p values form this fitted 906 distribution⁵⁰. * indicates significance at p < 0.05. 907

				CWM							CWV						
				r	nean		v	ariance			mean			varianc	е		
Trait	Abbreviation	TOP	Unit	obs.	SES	р	obs.	SES	р	obs.	SES	р	obs.	SES	р		
Leaf area	LA	25	mm ²	6.130	-9.75	*	1.691	12.53	*	1.565	-2.59	*	2.448	-0.27	n.s.		
Specific leaf area	SLA	50	m² kg⁻¹	2.850	9.89	*	0.172	12.88	*	0.150	-1.33	n.s.	0.023	1.10	n.s.		
Leaf fresh mass	Leaf.fresh.mass	35	g	-2.125	-13.28	*	1.395	10.83	*	1.520	-2.05	*	2.311	0.01	n.s.		
Leaf dry matter content	LDMC	45	g g⁻¹	-1.294	-5.67	*	0.101	11.52	*	0.130	0.95	n.s.	0.017	6.73	*		
Leaf C	LeafC	452	mg g⁻¹	6.116	-3.77	*	0.003	8.80	*	0.002	-1.78	*	0.000	-0.38	n.s.		
Leaf N	LeafN	462	mg g⁻¹	3.038	4.22	*	0.055	6.29	*	0.063	-3.19	*	0.004	-0.13	n.s.		
Leaf P	LeafP	463	mg g⁻¹	0.535	9.57	*	0.097	2.81	*	0.117	-5.17	*	0.014	-2.11	*		
Leaf N per area	LeafN.per.area	481	g m⁻²	0.251	-9.06	*	0.075	8.18	*	0.099	-0.28	n.s.	0.010	1.54	n.s.		
Leaf N:P ratio	Leaf.N:P.ratio	-	g g⁻¹	2.444	-11.95	*	0.040	0.40	n.s.	0.081	-2.74	*	0.007	-0.39	n.s.		
Leaf δ^{15} N	Leaf.delta15N	-	ppm	0.521	-3.58	*	0.254	6.68	*	0.455	2.82	*	0.207	2.44	*		
Seed mass	Seed.mass	103	mg	0.407	-11.19	*	2.987	3.69	*	2.784	-9.06	*	7.750	-2.81	*		
Seed length	Seed.length	91	mm	1.069	-4.51	*	0.294	5.50	*	0.365	-4.67	*	0.134	-3.07	*		
Seed number per reproductive unit	Seed.num.rep.unit	-		6.179	7.67	*	2.783	4.40	*	5.156	1.44	n.s.	26.588	2.25	*		
Dispersal unit length	Disp.unit.length	90	mm	1.225	-2.51	*	0.343	6.50	*	0.451	-3.21	*	0.203	-1.39	n.s.		

Plant height	Plant.height	68	m	-0.315	-12.15	*	1.532	13.34	*	1.259	-9.01	*	1.585	9.68	*
Stem specific density	SSD	286	g cm⁻³	-0.869	-14.93	*	0.041	13.15	*	0.058	2.09	*	0.003	2.99	*
Stem conduit density	Stem.cond.dens	-	mm⁻²	4.407	15.08	*	0.656	8.45	*	0.975	-0.95	n.s.	0.951	1.10	n.s.
Conduit element length	Cond.elem.length	-	μm	5.946	-7.09	*	0.182	9.14	*	0.367	7.12	*	0.135	5.29	*
Mean SES					-3.50			8.06			-1.76			1.25	
Mean absolute SES					8.66			8.06			3.36			2.43	

910 **Captions of Figures**

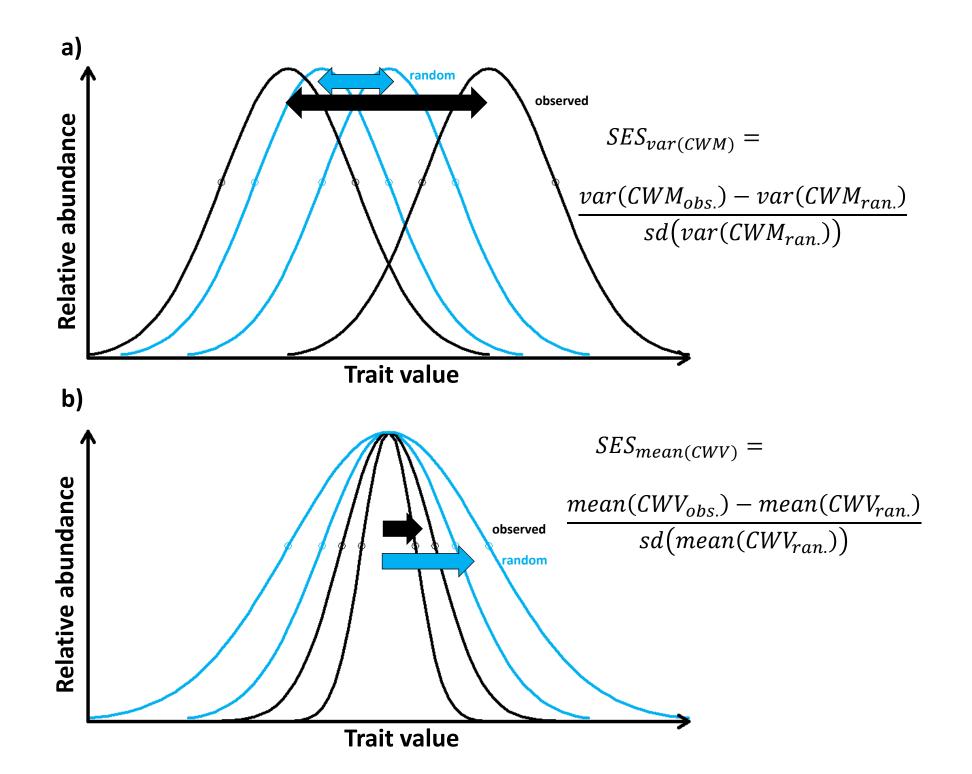
911

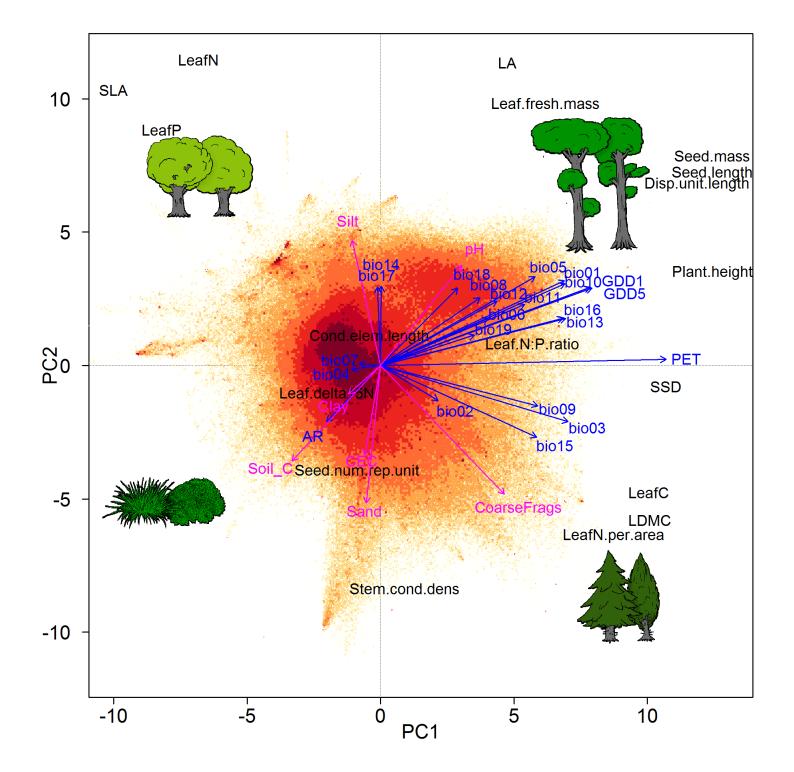
912 Fig. 1: Conceptual figure to illustrate Hypothesis 1, stating that environmental or biotic 913 filtering of community trait values result in a) higher than expected variation of community-914 weighted means and b) lower than expected community-weighted variances of trait values. 915 Both figures give an example for a single trait and show the relative abundance of trait values 916 of all species in a plot. Black curves refer to observed plot-level trait values in two exemplary 917 plots, while grey curves show plot-level trait values obtained from randomizing trait values 918 across all species globally (see Methods). Randomization was done 100 times, but only one 919 randomization event is shown. Deviation from random expectation was assessed with standardized effect sizes (SESs) for a) the variance in CWMs and b) for the mean in CWVs. 920 921 Evidence for filtering is given in a) if the variance in plot-level trait means was higher than expected by chance (SES significantly positive) or b) if within-plot trait variance was 922 typically lower than expected by chance (SES significantly negative, see Methods). 923 924 Fig. 2: Principal Component Analysis of global plot-level trait means (community-weighted means, CWMs). The plots (n=1,114,304) are shown by coloured dots, with shading indicating 925 926 plot density on a logarithmic scale, ranging from yellow with 1–4 plots at the same position to 927 dark red with 251-1142 plots. Prominent spikes are caused by a strong representation of communities with extreme trait values, such as heathlands with ericoid species with small leaf 928 area and seed mass. Post-hoc correlations of PCA axes with climate and soil variables are 929 930 shown in blue and magenta, respectively. Arrows are enlarged in scale to fit the size of the graph; thus, their lengths show only differences in variance explained relative to each other. 931 932 Variance in CWM explained by the first and second axis was 29.7% and 20.1%, respectively. 933 The vegetation sketches schematically illustrate the size continuum (short vs. tall) and the leaf 934 economics continuum (low vs. high LDMC and leaf N content per area in light and dark green 935 colours, respectively). See Table 2 and Supplementary Table 2 for the description of traits and 936 environmental variables.

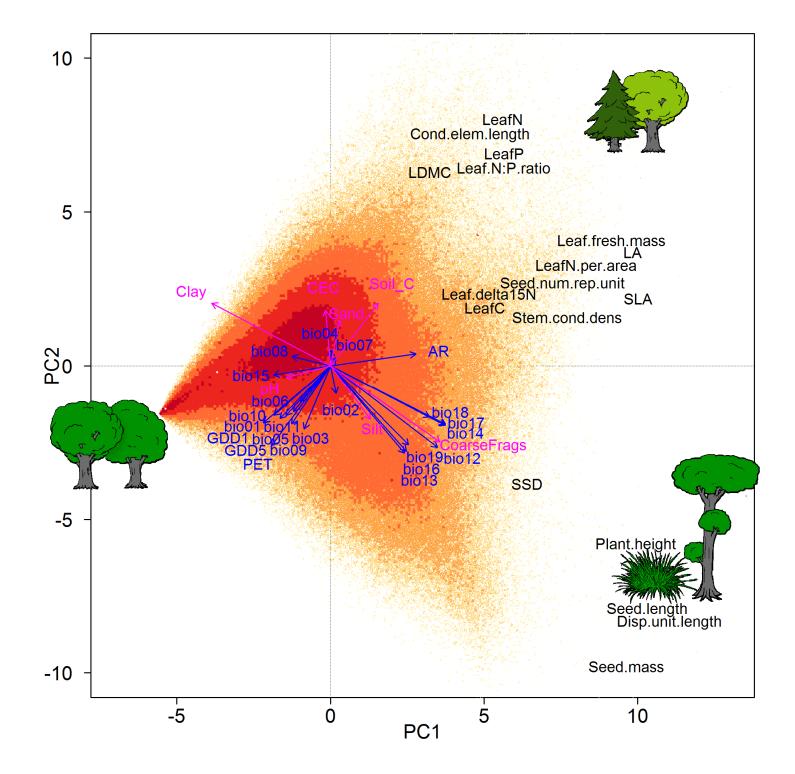
937

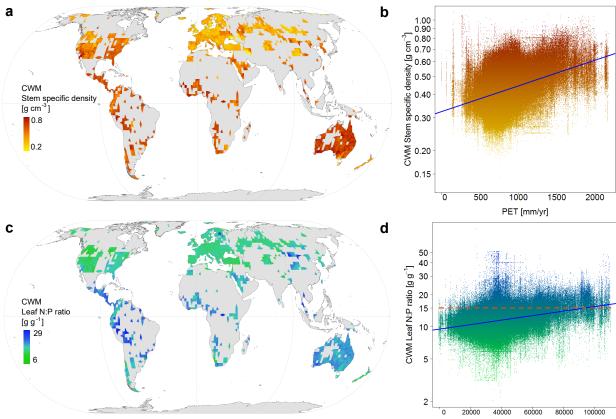
Fig. 3: Principal Component Analysis of global within-plot trait variances (community-938 weighted variances, CWVs). The plots (n=1,098,015) are shown by coloured dots, with 939 shading indicating plot density on a logarithmic scale, ranging from vellow with 1–2 plots at 940 941 the same position to dark red with 631–1281 plots. Post-hoc correlations of PCA axes with climate and soil variables are shown in blue and magenta, respectively. Arrows are enlarged 942 in scale to fit the size of the graph; thus, their lengths show only differences in variance 943 944 explained relative to each other. Variance in CWV explained by the first and second axis was 24.9% and 13.4%, respectively. CWV values of all traits increased from the left to the right, 945 which reflects increasing species richness ($r^2 = 0.116$ between scores of the first axis and 946 947 number of species in the communities for which traits were available). The vegetation 948 sketches schematically illustrate low and high variation in the plant size and leaf economics 949 continua. See Table 2 and Supplementary Table 2 for the description of traits and 950 environmental variables.

- 951
- 952 Fig. 4: The two strongest relationships found for global plot-level trait means (community-
- 953 weighted means, CWMs) in the sPlot dataset. CWM of the natural logarithm of stem specific
- 954 density [g cm⁻³] as a) global map, interpolated by kriging within a radius of 50 km around the
- 955 plots using a grid cell of 10 km, and b) function of potential evapotranspiration (PET,
- 956 $r^2=0.156$). CWM of the natural logarithm of the N:P ratio [g g⁻¹] as c) global kriging map and
- d) function of the warmth of the growing season, expressed as growing degree days over a
- threshold of 5°C (GDD5, $r^2=0.115$). Plots with N:P ratios > 15 (of 2.71 on the log_e scale) tend
- to indicate phosphorus limitation^{29'} and are shown above the broken line in red colour (90,979)
- 960 plots, 8.16% of all plots). The proportion of plots with N:P ratios > 15 increases with GDD5
- 961 ($r^2=0.895$ for a linear model on the log response ratio of counts of plots with N:P > 15 and
- 962 ≤ 15 counted within bins of 500 GDD5).









GDD5 [degree days]